

FRactal Dimensions of Random Water Surfaces

Michael STIASSNIE^a, Yehuda AGNON^a and Lev SHEMER^b

^aCoastal and Marine Engineering Research Institute, Department of Civil Engineering, Technion, Israel Institute of Technology, Haifa 32000, Israel

^bFaculty of Engineering, Tel-Aviv University, Tel-Aviv, Israel

Received 25 June 1990

Accepted 12 July 1990

Communicated by V.E. Zakharov

Fractal solutions of the inviscid water-wave problem are presented. For gravity waves (neglecting surface tension) free surfaces with fractal dimensions $2\frac{1}{4}$ and $2\frac{1}{3}$ are obtained. For capillary waves (neglecting gravity), subfractal free surfaces with dimension 2 are shown to exist. However, the situation is reversed if one considers time series of the surface elevation taken at a fixed point. In this case the capillary wave solution produces graphs with dimension $1\frac{1}{12}$, whereas the graph for gravity waves has dimension 1.

1. Main ideas and results

1.1. Random surfaces

Homogeneous random surfaces $z = \eta(\mathbf{x}) = \eta(x, y)$ are usually specified in terms of their wavenumber spectrum $\Psi(\mathbf{k}) = \Psi(k_x, k_y)$, which is the Fourier transform of the covariance of the surface displacement η

$$\Psi(\mathbf{k}) = \frac{1}{(2\pi)^2} \int_r \overline{\eta(\mathbf{x}) \eta(\mathbf{x} + \mathbf{r})} e^{-i\mathbf{k} \cdot \mathbf{r}} d\mathbf{r}. \quad (1.1)$$

Assuming η to be a multivariate Gaussian process there is a way to retrieve η from Ψ through

$$\eta(\mathbf{x}) = \int_k a(\mathbf{k}) \cos[\mathbf{k} \cdot \mathbf{x} + \chi(\mathbf{k})] \sqrt{2\Psi(\mathbf{k})} d\mathbf{k}. \quad (1.2)$$

Here $\chi(\mathbf{k}) = \epsilon(\mathbf{k})$ are random phase shifts having a rectangular distribution over the range $(-\pi, \pi)$; and $a(\mathbf{k})$ are independent random amplitudes with unit mean.

1.2. Water surfaces

In the case of a free surface of a heavy fluid such as water, η is also a function of time t , and the components in (1.2) are referred to as waves. If the nonlinear interactions among these waves are weak enough the wave frequency ω is related to the wavenumber \mathbf{k} through the linear dispersion relation

$$\omega^2 = gk + sk^3, \quad (1.3)$$

where $k = |\mathbf{k}|$, g is the gravitational acceleration, and s is the ratio between the surface tension coefficient and the density of the liquid. In this case (1.2) still applies, but the phase becomes time dependent: $\chi(\mathbf{k}) = \epsilon(\mathbf{k}) - \omega(\mathbf{k})t$. In the sequel we refer to ‘pure’ gravity waves (denoted by subscript g) and to ‘pure’ capillary waves (with subscript c). For these two extreme cases (1.3) is rewritten as

$$\omega/\omega_* = (k/k_*)^\gamma \quad (1.4a)$$

where the asterisk is used for scaling, and

$$\gamma_g = 1/2, \quad \gamma_c = 3/2. \quad (1.4b)$$

For water surfaces Srokosz [12] assumes that the amplitudes in (1.2) are Rayleigh distributed on $(0, \infty)$ with mean 1; whereas Pierson [11] and Kinsman [5] choose $a(\mathbf{k}) \equiv 1$. In the sequel we adopt the second choice, which simplifies the mathematical presentation but does not affect the generality of our results.

1.3. Dynamical evolution of free surfaces

The dynamics of a wave field is conveniently described by the balance of action spectral density $N(\mathbf{k}, t)$, governed by the weakly nonlinear interaction of resonating wave-triads (I_T) and wave-quartets (I_Q):

$$\frac{\partial N}{\partial t} = I_T + I_Q, \quad (1.5)$$

$$\begin{aligned} I_T = & 16\pi^3 \int \int \{ N(\mathbf{k}_1) N(\mathbf{k}_2) - N(\mathbf{k}) [N(\mathbf{k}_1) + N(\mathbf{k}_2)] \} \\ & \times [V^{(-)}(\mathbf{k}, \mathbf{k}_1, \mathbf{k}_2)]^2 \delta(\mathbf{k} - \mathbf{k}_1 - \mathbf{k}_2) \delta(\omega - \omega_1 - \omega_2) \\ & + 2\{ N(\mathbf{k}_2) [N(\mathbf{k}) + N(\mathbf{k}_1)] - N(\mathbf{k}) N(\mathbf{k}_1) \} \\ & \times [V^{(-)}(\mathbf{k}_2, \mathbf{k}_1, \mathbf{k})]^2 \delta(\mathbf{k} + \mathbf{k}_1 - \mathbf{k}_2) \delta(\omega + \omega_1 - \omega_2) \} d\mathbf{k}_1 d\mathbf{k}_2, \end{aligned} \quad (1.6a)$$

$$\begin{aligned} I_Q = & 64\pi^5 \int \int \int \{ N(\mathbf{k}_2) N(\mathbf{k}_3) [N(\mathbf{k}) + N(\mathbf{k}_1)] - N(\mathbf{k}) N(\mathbf{k}_1) [N(\mathbf{k}_2) + N(\mathbf{k}_3)] \} \\ & \times [T(\mathbf{k}, \mathbf{k}_1, \mathbf{k}_2, \mathbf{k}_3)]^2 \delta(\mathbf{k} + \mathbf{k}_1 - \mathbf{k}_2 - \mathbf{k}_3) \delta(\omega + \omega_1 - \omega_2 - \omega_3) d\mathbf{k}_1 d\mathbf{k}_2 d\mathbf{k}_3. \end{aligned} \quad (1.6b)$$

The kernels $V^{(-)}$ and T can be found in ref. [3].

It is well known that ‘pure’ gravity waves do not undergo triad resonant interactions ($I_T \equiv 0$) and that for this case I_Q becomes the leading term on the r.h.s. of eq. (1.5). Capillary waves, however, are subject to triad and quartet resonances, but the first usually dominates and I_Q is often disregarded. Hasselmann [2] and Valenzuela and Laing [15] were the first to derive I_Q and I_T respectively (cf. also refs. [4, 16]).

We have rederived both expressions by starting from the Zakharov equation (cf. refs. [14, 18, 19] and using the methodology originally applied by Longuet-Higgins [8] to the cubic Schrödinger equation. Details of derivation of I_T have been omitted. The derivation is similar to the way that I_Q is derived in ref. [13].

It can be shown that the wavenumber spectrum $\Psi(\mathbf{k})$ is related to the action density $N(\mathbf{k})$ by

$$\Psi(\mathbf{k}) = [N(\mathbf{k}) + N(-\mathbf{k})] k/2\omega. \quad (1.7)$$

1.4. Stationary solutions

Zakharov and Filonenko [20] found that the equation $dN/dt = I_Q$ for ‘pure’ gravity waves has two stationary solutions

$$N/N_* = (k_*/k)^{\bar{\alpha}} \tag{1.8}$$

with $\bar{\alpha} = \bar{\alpha}_g = 23/6, 4$ (cf. also ref. [22]).

In a similar way we have proved that the equation $dN/dt = I_T$ for ‘pure’ capillary waves has a solution of the same nature as (1.8), but with $\bar{\alpha} = \bar{\alpha}_c = 17/4$.

The result for capillary waves was derived earlier by Zakharov and Filonenko [21]^{#1}.

From (1.7) and (1.8) we obtain

$$\Psi/\Psi_* = (k_*/k)^{\bar{\alpha}}, \tag{1.9}$$

where $\bar{\alpha}_g = 10/3, 7/2$ and $\bar{\alpha}_c = 19/4$. For these cases (1.2) becomes

$$\eta(\mathbf{x}, t) = \eta_* \int_0^\infty \int_{-\pi}^\pi \cos\{k(\omega)[x \cos \theta + y \sin \theta] - \omega t + \epsilon(\omega, \theta)\} (\omega_*/\omega)^{\beta_{1/2}} \sqrt{d(\omega/\omega_*)} d\theta, \tag{1.10a}$$

where

$$\beta_{1g} = 11/3, 4 \quad \text{and} \quad \beta_{1c} = 17/6. \tag{1.10b}$$

1.5. Time series and instantaneous sections

Pierson [11] has shown that for a sea surface given by (1.10) the local variation of η with time, at any fixed point $\mathbf{x} = \mathbf{x}_0$, is written as

$$\eta(t) = \sqrt{2\pi} \eta_* \int_0^\infty \cos[\omega t + \epsilon(\omega)] (\omega_*/\omega)^{\beta_{1/2}} \sqrt{d(\omega/\omega_*)} d\omega. \tag{1.11}$$

The three-dimensional stationary Gaussian process (1.10) can also be reduced to another one-dimensional process, similar to (1.11), if one looks at the wave pattern along any given line at any instant. If the distance along this line is denoted by ζ , then following Pierson we get

$$\eta(\zeta) = \eta_* \int_0^\infty \cos[k\zeta + \epsilon(k)] \sqrt{F(k) d(k/k_*)} dk, \tag{1.12}$$

where

$$F(k) = k_* \int_{-\pi}^\pi \left(\frac{k_*}{k} |\cos \alpha|\right)^{\gamma \beta_1} \frac{2\gamma k^{\gamma-1}}{(k_* |\cos \alpha|)^\gamma} d\alpha \tag{1.13a}$$

^{#1}We are grateful to the referee who brought this to our attention. Since the original reference [21] is not easily accessible, we give our brief derivation in the appendix.

with γ given in (1.4b) and β_1 in (1.10b).

$$F(k) = 2\gamma \left(\frac{k_*}{k}\right)^{\beta_2} \int_{-\pi}^{\pi} |\cos \alpha|^{\gamma(\beta_1-1)} d\alpha = 4\gamma \left(\frac{k_*}{k}\right)^{\beta_2} B\left(\frac{1}{2}, \frac{1}{2}\beta_2\right), \tag{1.13b}$$

where B is the beta function (see e.g. ref. [10], eq. 3.5) and

$$\beta_2 = 1 + \gamma(\beta_1 - 1). \tag{1.14}$$

Substitution of (1.13b) into (1.12) yields

$$\eta(\zeta) = 2\eta_* \sqrt{\gamma B\left(\frac{1}{2}, \frac{1}{2}\beta_2\right)} \int_0^\infty \cos[k\zeta + \epsilon(k)] \left(\frac{k_*}{k}\right)^{\beta_2/2} \sqrt{d(k/k_*)}. \tag{1.15a}$$

From (1.4b), (1.10b) and (1.14) we obtain

$$\beta_{2g} = 7/3, 5/2 \quad \text{and} \quad \beta_{2c} = 15/4. \tag{1.15b}$$

1.6. Fractal dimensions of the free surface

In section 2 we prove that the graph of

$$V(t) = \int_0^\infty \cos(\omega t + \epsilon) \sqrt{S(\omega)} d\omega, \quad S(\omega) = \omega^{-\beta}$$

has a fractal dimension D related to β by

$$D = (5 - \beta)/2. \tag{1.16}$$

Substituting (1.10b) and (1.15b) into (1.16) yields the values for D given in table 1. We note that values of D in the range between 1 to 2 correspond to *fractals* with dimension D whereas values between 0 to 1 correspond to *subfractals*, namely graphs of dimension 1 having a fractal derivative with dimension $1 + D$. The dimension of the free surface itself for gravity waves is $D + 1 = 2\frac{1}{3}, 2\frac{1}{4}$, whereas for capillary waves it is 2. On the other hand, the dimension of the time series for gravity waves is $D = 1$, whereas for capillary waves $D = 1\frac{1}{2}$.

2. Fractal dimension and $1/\omega^\beta$ spectra

The goal of the present section is to provide a proof for eq. (1.16), which relates the fractal dimension D to the exponent of the spectrum β .

Table 1
Calculated values of D

	Gravity waves	Capillary waves
time series	2/3, 1/2	13/12
instantaneous sections	4/3, 5/4	5/8

Corollary 2.1. The following two stochastic processes,

$$(a) \quad V(t) = \int_0^\infty \cos(\omega t + \epsilon) \sqrt{S(\omega)} d\omega, \quad S = \omega^{-\beta}; \tag{2.1}$$

and (b) the ‘fractional Brownian motion’ [17],

$$V_H(t) = \frac{1}{\Gamma(H + 1/2)} \int_{-\infty}^t (t - s)^{H-1/2} W(s) ds, \tag{2.2}$$

where $W(s)$ is a Gaussian white noise, are identical provided that

$$\beta = 2H + 1. \tag{2.3}$$

Proof. First, we write the white noise $W(s)$ in a form similar to (2.1)

$$W(s) = \int_0^\infty \cos(\omega s + \epsilon) \sqrt{d\omega}. \tag{2.4}$$

Second, we note that (2.2) is actually

$$V_H = {}_{-\infty}I_t^{H+1/2} W, \tag{2.5}$$

where ${}_{-\infty}I_x^\nu$ is the fractional integration operator due to Liouville and Riemann, see ref. [9]:

$${}_{-\infty}I_x^\nu f(x) = \frac{1}{\Gamma(\nu)} \int_{-\infty}^x f(t) (x - t)^{\nu-1} dt. \tag{2.6}$$

Third, changing the order of integration and applying Mikolas’ results [9] for fractional integration of sine and cosine functions we get

$$\begin{aligned} V_H &= {}_{-\infty}I_t^{H+1/2} \int_0^\infty \cos(\omega t + \epsilon) \sqrt{d\omega} = \int_0^\infty \sqrt{d\omega} {}_{-\infty}I_t^{H+1/2} \cos(\omega t + \epsilon) \\ &= \int_0^\infty \sqrt{d\omega} \cos[\omega t - (H + 1/2)\pi/2 + \epsilon] \omega^{-(H+1/2)} = \int_0^\infty \cos[\omega t + \tilde{\epsilon}] \sqrt{\omega^{-(2H+1)}} d\omega. \end{aligned} \tag{2.7}$$

Last, comparing the result in (2.7) with (2.1), we obtain (2.3).

Corollary 2.2. The process $V = V_H$ is self-affine, i.e.

$$\Delta V_H(r \Delta t) = r^H \Delta V_H(\Delta t). \tag{2.8}$$

Proof.

$$\Delta V_H(\Delta t) = V_H(t_2) - V_H(t_1) = \frac{1}{\Gamma(H + 1/2)} \int_{t_1}^{t_2} (t - s)^{H-1/2} W(s) ds, \tag{2.9}$$

$$\Delta V_H(r \Delta t) = V_H(rt_2) - V_H(rt_1) = \frac{1}{\Gamma(H + 1/2)} \int_{rt_1}^{rt_2} (rt - s)^{H-1/2} W(s) ds, \tag{2.10}$$

changing the integration variable in (2.10) to $S = s/r$ and applying the relation $W(rS) = r^{-1/2}W(S)$ yields

$$\Delta V_H(r \Delta t) = \frac{r^H}{\Gamma(H + 1/2)} \int_{t_1}^{t_2} (t - S)^{H-1/2} W(S) dS. \tag{2.11}$$

Comparing (2.11) with (2.9) produces (2.8).

Corollary 2.3. The fractal dimension (capacity) of $V = V_H$ is

$$D = 2 - H. \tag{2.12}$$

Proof. First we scale t and $V_H(t)$ so that initially $\Delta t = 1$, and $\Delta V_H(\Delta t) = 1$, see fig. 1.

Second, we divide the range $\Delta t = 1$ into M equal parts, each $r = 1/M$ units wide. The vertical extent l needed in order to cover the graph V_H is determined by the property of affinity and is given by $l = 1/M^H$. Thus, the vertical column comprises $n \approx M^{-H+1}$ r by r squares. The total number of such squares needed to cover that part of the graph which was originally covered by the 1 by 1 square is $N = Mn = M^{2-H} \approx r^{H-2}$.

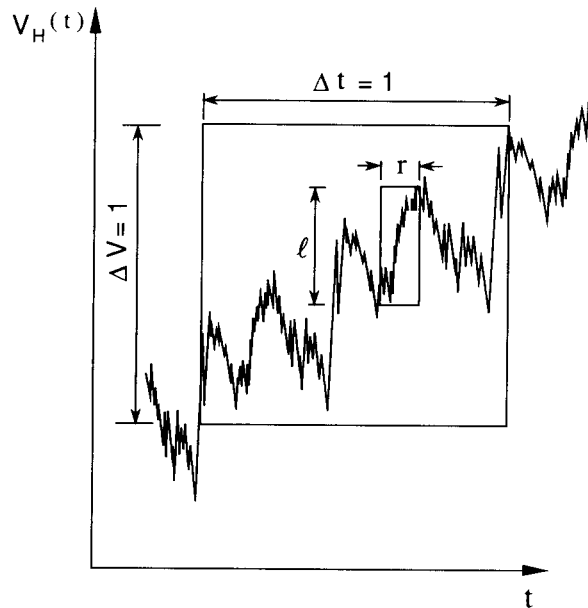


Fig. 1. Covering V_H with squares.

Third, calculating the capacity, as originally defined by Kolmogorov [6]:

$$D = \lim_{r \rightarrow 0} \frac{\log N(r)}{\log(r^{-1})} = \frac{\log(r^{H-2})}{\log(r^{-1})} = 2 - H. \quad (2.13)$$

Last, we note that the term ‘fractal dimension’ was coined by Mandelbrot, who used it as a synonym for the Hausdorff dimension. Other authors use the term ‘fractal dimension’ as a synonym for capacity. Nevertheless, for many examples the capacity and the Hausdorff dimension take on a common value.

Eq. (1.16) is obtained by eliminating H from (2.3) and (2.12).

3. Discussion of naturally generated waves

In addressing the question of the relevance of our findings to naturally generated waves, we consider the following:

- (1) The existence of equilibrium ranges with appropriate power law spectra.
- (2) The azimuthal dependence of wave spectra.
- (3) The range of scales over which these power laws apply.

3.1. Power law spectra

The wave action spectral density balance equation includes terms due to action exchange among different wavenumbers by nonlinear interaction as well as growth due to the wind and dissipation by wave breaking (for gravity waves) and viscous effects (in capillary waves).

It is remarkable that even though we have not taken into account the wind input and dissipation, the exponents obtained agree well with reported measurements.

For gravity waves, Phillips [10] summarizes several field and laboratory experiments. His results agree exactly with the value $\bar{\alpha}_g = 3.5$ of eq. (1.9). The other theoretical value, $\bar{\alpha}_g = 3.33$, seems too close to the first one to make it possible to distinguish between them experimentally.

For capillary waves generated in a wind-wave tunnel Leonart and Blackman [7] obtained results that correspond to $\bar{\alpha}_c = 5$. This is very close to our result of $\bar{\alpha}_c = 4.75$.

It is quite likely that in the range considered (see section 3.3), nonlinear wave–wave interaction are dominant especially when compared with the combined effect of wind input and dissipation. Van Gastel [16] has computed the time scales for the different processes and has reached this conclusion.

3.2. Angular spread

We have considered equilibrium spectra which are isotropic. Unidirectional spectra can also be derived (cf. ref. [13]). A more general form, widely used, is that of a product of a frequency-dependent function and an azimuth-dependent one. We note that recent measurements of two-dimensional spectra of short gravity wind waves (0.2–1.6 m) by Banner et al. [1] clearly indicate a uniform angular distribution of energy. If one wishes to consider spectra which have the form of a power of the frequency times an angular factor, the derivation of the fractal dimension follows through, regardless of the angular spread.

3.3. Domain of applicability

It is clear that no natural object can be an ideal fractal any more than it can be completely smooth. The usefulness of the fractal description is related to the ranges of scales over which the power law spectra apply. We do not expect them to apply for scales on which wind input and dissipation become dominant, nor in the intermediate range of gravity–capillary waves, where the dispersion relation is not well approximated by power laws. For gravity waves Phillips [10] suggests a good agreement with the power law for wavelengths in the range between 0.1 and about 15 m, which gives a scale ratio of approximately 2^7 . For capillary waves Leonart and Blackman's measurements [7] suggest that the power law applies for wavelengths between about 2 mm and 1.6 cm (1.6 cm being already in the gravity–capillary range), giving a scale ratio of 2^3 .

Acknowledgement

This study is supported by the US Office of Naval Research under Grant No. N00014-88-J-1027.

Appendix. Equilibrium of capillary waves

The evolution equation for capillary waves can be written in terms of N as

$$\begin{aligned} \frac{dN}{dt} = & 16\pi^3 \iint \left\{ (V_{012}^{(-)})^2 [N_1 N_2 - N(N_1 + N_2)] \delta(\mathbf{k} - \mathbf{k}_1 - \mathbf{k}_2) \delta(\omega - \omega_1 - \omega_2) \right. \\ & \left. + 2(V_{210}^{(-)})^2 [N_2(N + N_1) - NN_1] \delta(\mathbf{k} + \mathbf{k}_1 - \mathbf{k}_2) \delta(\omega + \omega_1 - \omega_2) \right\} d\mathbf{k}_1 d\mathbf{k}_2. \end{aligned} \quad (\text{A.1})$$

For a steady state solution, the r.h.s. of (A.1) equals zero. Following Zakharov and Filonenko [20], we look for isotropic solutions in the form

$$N(\mathbf{k}) = N(k). \quad (\text{A.2})$$

Using polar coordinates for the wavenumbers and averaging (A.1) over the angles, we obtain

$$\begin{aligned} k \frac{dk}{d\omega} \int_0^{2\pi} \frac{dN}{dt} d\theta = & \iint_0^\infty [S_{012}(N_1 N_2 - NN_1 - NN_2) \delta(\omega - \omega_1 - \omega_2) \\ & + 2S_{201}(NN_2 + N_1 N_2 - NN_1) \delta(\omega + \omega_1 - \omega_2)] d\omega_1 d\omega_2, \end{aligned} \quad (\text{A.3})$$

where

$$S_{012} = 16\pi^3 k k_1 k_2 \frac{dk}{d\omega} \frac{dk_1}{d\omega_1} \frac{dk_2}{d\omega_2} \iint_0^{2\pi} (V_{012}^{(-)})^2 \delta(\mathbf{k} - \mathbf{k}_1 - \mathbf{k}_2) d\theta d\theta_1 d\theta_2 \quad (\text{A.4})$$

and N is taken as a function of ω . Note that $S_{012} = S_{021}$ since $V_{012}^{(-)} = V_{021}^{(-)}$. S is homogeneous in ω of degree $8/3$, i.e. for any positive α :

$$S(\alpha\omega, \alpha\omega_1, \alpha\omega_2) = \alpha^{8/3}S(\omega, \omega_1, \omega_2), \tag{A.5}$$

since for ‘pure’ capillary waves $V^{(-)}$ is homogeneous in k of degree $9/4$, and k is proportional to $\omega^{2/3}$.

Due to the delta functions, the integration over the (ω_1, ω_2) plane in the r.h.s. of (A.3) can be reduced into line integrals. There is a correspondence among triads in the two terms in eq. (A.3), through permutations of indices, which coincides with the appropriate symmetry of the interaction coefficients, S . We divide the domain of integration for the first term into two integrals, I_1 and I_2 , and the second into I_3 and I_4 . We then map each of the domains onto the domain of I_1 , making use of the homogeneity of S and the isotropy of N :

$$k \frac{dk}{d\omega} \frac{d}{dt} \int_0^{2\pi} N d\theta = \sum_{n=1}^4 I_n, \tag{A.6}$$

where

$$I_1 = \int_0^{\omega/2} d\omega_2 S_{0,0-2,2}(N_{0-2}N_2 - NN_{0-2} - NN_2), \tag{A.6a}$$

$$I_2 = \int_0^{\omega/2} d\omega_1 S_{0,1,0-1}(N_1N_{0-1} - NN_1 - NN_{0-1}), \tag{A.6b}$$

$$I_3 = 2 \int_0^{\omega} d\omega_1 S_{0+1,0,1}(NN_{0+1} - N_1N_{0+1} - NN_1), \tag{A.6c}$$

$$I_4 = 2 \int_{2\omega}^{\infty} d\omega_2 S_{2,0,2-0}(NN_2 + N_{2-0}N_2 - NN_{2-0}), \tag{A.6d}$$

where $i - j$ stands for l , such that $\omega_l = \omega_i - \omega_j$. The paths of integration in the (ω_1, ω_2) plane are shown in fig. 2.

Changing the variables of integration in (A.6a)–(A.6d) as follows:

$$(A.6a): \quad \omega_2 = \zeta,$$

$$(A.6b): \quad \omega_1 = \zeta,$$

$$(A.6c): \quad \omega_1 = \alpha_c \zeta, \quad \alpha_c = \omega / (\omega - \zeta), \quad d\omega_1 = \alpha_c^2 d\zeta,$$

$$(A.6d): \quad \omega_2 = \alpha_d \omega, \quad \alpha_d = \omega / \zeta, \quad d\omega_2 = -\alpha_d^2 d\zeta,$$

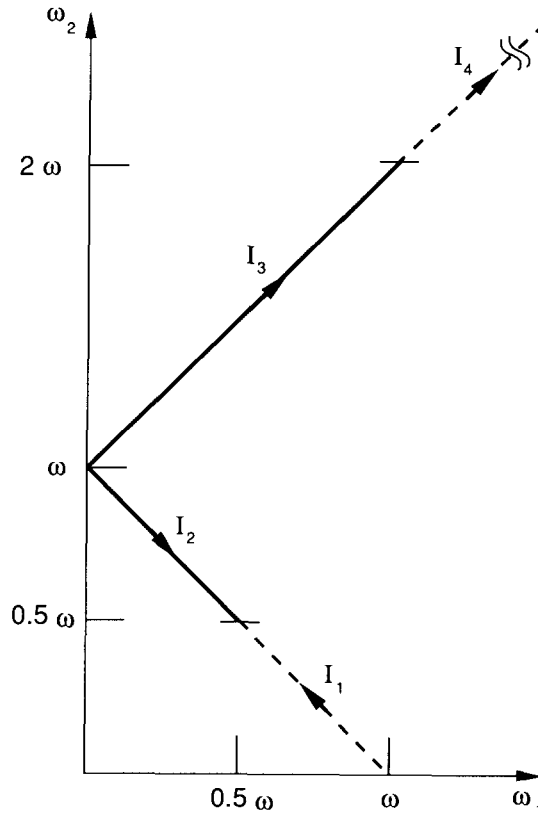


Fig. 2. Integration path.

and rewriting (A.6a)–(A.6d) in the new variables of integration and applying (A.5) yields:

$$I_1 + I_2 = 2 \int_0^{\omega/2} d\zeta S(\omega, \omega - \zeta, \zeta) [N(\omega - \zeta) N(\zeta) - N(\omega) N(\omega - \zeta) - N(\omega) N(\zeta)],$$

$$I_3 = 2 \int_0^{\omega/2} d\zeta \alpha_c^{14/3} S(\omega, \omega - \zeta, \zeta) \times [N(\alpha_c(\omega - \zeta)) N(\alpha_c \omega) + N(\alpha_c \zeta) N(\alpha_c \omega) - N(\alpha_c(\omega - \zeta)) N(\alpha_c \zeta)],$$

$$I_4 = 2 \int_0^{\omega/2} d\zeta \alpha_d^{14/3} S(\omega, \zeta, \omega - \zeta) \times [N(\alpha_d \zeta) N(\alpha_d \omega) + N(\alpha_d(\omega - \zeta)) N(\alpha_d \omega) - N(\alpha_d \zeta) N(\alpha_d(\omega - \zeta))].$$

Substitution of the above into (A.6) and assuming

$$N(\omega) = N_*(\omega/\omega_*)^x \tag{A.7}$$

gives

$$k \frac{dk}{d\omega} \frac{d}{dt} \int_0^{2\pi} N d\theta = \frac{2N_*^2}{\omega_*^{2x}} \int_0^{\omega/2} d\zeta S(\omega, \zeta, \omega - \zeta) \left[\zeta^x (\omega - \zeta)^x - \omega^x (\omega - \zeta)^x - \omega^x \zeta^x \right] \\ \times \left[\zeta^{14/3+2x} (\omega - \zeta)^{14/3+2x} - \omega^{14/3+2x} (\omega - \zeta)^{14/3+2x} - \omega^{4/3+2x} \zeta^{14/3+2x} \right]. \quad (\text{A.8})$$

The first of the expressions in square brackets is equal to zero for $x = -1$, and the second for $14/3 + 2x = -1$, i.e. for $x = -17/6$. The solution $x = -1$ implies a uniform energy density and is less interesting. The spectrum

$$N = N_* (\omega/\omega_*)^{-17/6} \quad (\text{A.9})$$

can be viewed as an approximate solution for the high-frequency range, which is dominated by capillarity.

The wave action flux $p(\omega)$ and the wave energy flux $q(\omega)$ satisfy

$$\frac{\partial p}{\partial \omega} = -k \frac{dk}{d\omega} \frac{\partial N}{\partial t}, \quad (\text{A.10a})$$

$$\frac{\partial q}{\partial \omega} = -k \frac{dk}{d\omega} \omega \frac{\partial N}{\partial t}. \quad (\text{A.10b})$$

Since $(\partial N/\partial t)k(dk/d\omega)$ was found to be homogeneous in ω of order $(11/3 + 2x)$, p and q are homogeneous in ω of orders $(14/3 + 2x)$ and $(17/3 + 2x)$, respectively, yielding for $x = -17/6$; $p = p_*/\omega$, $q = q_*$. From eq. (A.3) we see that N_* is proportional to $q_*^{1/2}$.

For equilibrium, (A.10a) dictates $p_* = 0$. To find the direction of the energy flux q , we examine the interaction of a single resonant triad, $\mathbf{k} = \mathbf{k}_1 + \mathbf{k}_2$. From (A.1) we see that wave action is added to $N(k)$ at a rate

$$32\pi^3 V^{(1)} [N_1 N_2 - N(N_1 + N_2)] \equiv \Delta N, \quad (\text{A.11})$$

which is positive for $x = -17/6$. $N(k_1)$ and $N(k_2)$ decrease each at that same rate, so together they lose twice the wave action that $N(k)$ receives. Thus, wave action is only conserved over the whole spectrum but not for each triad separately. In contrast, for any spectrum, energy and momentum are conserved within each triad:

$$\Delta N \omega = \Delta N \omega_1 + \Delta N \omega_2, \quad (\text{A.12a})$$

$$\Delta N \mathbf{k} = \Delta N \mathbf{k}_1 + \Delta N \mathbf{k}_2 \quad (\text{A.12b})$$

since $\omega = \omega_1 + \omega_2$, $\mathbf{k} = \mathbf{k}_1 + \mathbf{k}_2$. Thus it is clear that the energy flux is directed to higher wavenumbers, where it can be dissipated by viscosity.

References

- [1] M.L. Banner, I.S.F. Jones and J.C. Trinder, Wavenumber spectra of short gravity waves, *J. Fluid Mech.* 198 (1989) 321–344.
- [2] K. Hasselmann, On the nonlinear energy transfer in a gravity-wave spectrum. 1. General theory, *J. Fluid Mech.* 12 (1962) 481–500.
- [3] S.J. Hogan, I. Gruman and M. Stiassnie, On the change in phase speed of one train of water waves in the presence of another, *J. Fluid Mech.* 192 (1988) 97–114.
- [4] D. Holliday, On nonlinear interactions in spectra of inviscid gravity–capillary surface waves, *J. Fluid Mech.* 83 (1977) 737–749.
- [5] B. Kinsman, *Wind waves, their generation and propagation on the ocean surface* (Prentice-Hall, Englewood Cliffs, NJ, 1965) 676 p.
- [6] A.N. Kolmogorov, A new invariant for transitive dynamical systems, *Dokl. Acad. Nauk. SSSR* 119 (1958) 861–864.
- [7] G.T. Leonart and D.R. Blackman, The spectral characteristics of wind-generated capillary waves, *J. Fluid Mech.* 97 (1980) 455–479.
- [8] M.S. Longuet-Higgins, On the nonlinear transfer of energy in the peak of a gravity-wave spectrum: A simplified model, *Proc. R. Soc. London A* 347 (1976) 311–328.
- [9] M. Mikolas, On the recent trends in the development, theory and applications of fractional calculus, in: *Fractional Calculus and its Applications*, ed. B. Ross, *Lecture Notes in Mathematics*, No. 457 (Springer, Berlin, 1975) pp. 357–375.
- [10] O.M. Phillips, Spectral and statistical properties of the equilibrium range in wind-generated gravity waves, *J. Fluid Mech.* 156 (1985) 505–531.
- [11] W.J. Pierson, Wind generated gravity waves, *Adv. Geophys.* 2 (1955) 93–178.
- [12] M.A. Srokosz, On the joint distribution of surface elevation and slopes for a nonlinear sea, with an application to radar altimetry, *J. Geophys. Res.* 91, No. C1 (1986) 995–1006.
- [13] M. Stiassnie, The fractal dimension of the ocean surface, in: *Nonlinear Topics in Ocean Physics, Proceedings of the International School of Physics, Enrico Fermi, 1988*, in press.
- [14] M. Stiassnie and L. Shemer, On modifications of the Zakharov equation for surface gravity waves, *J. Fluid Mech.* 143 (1984) 47–67.
- [15] G.R. Valenzuela and M.B. Laing, Nonlinear energy transfer in gravity–capillary wave spectra, with applications, *J. Fluid Mech.* 54 (1972) 507–520.
- [16] K. Van Gastel, Nonlinear interaction of gravity capillary waves: Lagrangian theory and effects on the spectrum, *J. Fluid Mech.* 182 (1987) 499–523.
- [17] R.F. Voss, Fractals in nature: From characterization to simulation, in: *The Science of Fractal Images*, eds. H.-O. Peitgen and D. Saupe (Springer, Berlin, 1988) pp. 21–70.
- [18] H.C. Yuen and B.M. Lake, Nonlinear dynamics of deep-water gravity waves, *Adv. Appl. Mech.* 22 (1982) 67–229.
- [19] V.E. Zakharov, Stability of periodic waves of finite amplitude on the surface of a deep fluid, *J. Appl. Mech. Tech. Phys.* 2 (1968) 190–194.
- [20] V.E. Zakharov and N.N. Filonenko, Energy spectrum for stochastic oscillations of the surface of a liquid, *Sov. Phys. Dokl.* 170 (1966) 1292–1295 [English transl., *Sov. Phys. Dokl.* 11 (1967) 881–883].
- [21] V.E. Zakharov and N.N. Filonenko, Weak turbulence of capillary waves, *Prikl. Mekh. Tekh. Fiz.* 8(5) (1967) 62–67 (in Russian).
- [22] V.E. Zakharov and M.M. Zaslavskii, The kinetic equation and Kolmogorov spectra in the weak turbulence theory of wind waves, *Izv. Atmos. Oceanic Phys.* 18 (1982) 747–753.